Analyst

Cite this: *Analyst*, 2012, **137**, 4577

www.rsc.org/analyst

PAPER

Highly sensitive and selective dopamine biosensor based on a phenylethynyl ferrocene/graphene nanocomposite modified electrode†

Meiling Liu,[a] Linping Wang,[a] Jianhui Deng,[a] Qiong Chen,[a] Yuzhen Li,[a] Youyu Zhang,[a] Haitao Li*[ab] and Shouzhuo Yao*[a]

Received 29th May 2012, Accepted 1st August 2012
DOI: 10.1039/c2an35708a

A new ferrocene derivative (1-[(4-amino) phenylethynyl]ferrocene, Fc-NH_2) was synthesized for the first time. The ferrocene derivative molecule contained the phenylethynyl skeleton, ferrocene and amino groups with excellent electrochemical properties. The graphene/Fc-NH_2 nanocomposite was prepared by mixing graphene solution and Fc-NH_2 solution in one pot and the nanocomposite was utilized to construct a Nafion/graphene/Fc-NH_2 modified glassy carbon electrode (GCE). The ferrocene derivative immobilized on the graphene can enhance the charge-transport ability of the nanocomposite, stabilize the graphene and prevent the leakage of ferrocene. The detection signal of dopamine (DA) was significantly amplified on the Nafion/graphene/Fc-NH_2/GCE. It was experimentally demonstrated that the signal enhancement results from the synergy amplification effect of graphene and the Fc-NH_2. The oxidation peak currents of DA were linearly related to the concentrations in the range of 5×10^{-8} to 2×10^{-4} M with the detection limit of 20 nM in the absence of uric acid (UA) and ascorbic acid (AA). In the presence of 10^{-3} M AA and 10^{-4} M UA, the linear response range was 1×10^{-7} to 4×10^{-4} M, and the detection limit was 50 nM at $S/N = 3$. Using the proposed Nafion/Fc-NH_2/graphene/GCE, DA was successfully determined in real samples with the standard addition method.

1. Introduction

Dopamine (DA) is one of the most important neurotransmitters in the mammalian central nervous system. A change in the level of DA has been proven to be effective toward brain functions.[1,2] It was reported that the loss of DA-containing neurons may result in serious diseases, such as Parkinson's disease. Thus sensitive and selective detection of DA is very important in life science. Many methods, such as liquid chromatography,[3,4] chemiluminescence,[5,6] capillary electrophoresis,[7] fluorescence,[8] absorbance and colorimetric,[9] and electrochemical methods,[10,11] have been successfully developed to detect DA. Apparently, all the methods mentioned above are effective in DA detection. Among these methods, the electrochemical technique has been proved to be one of the most advantageous methods in the determination of DA.[1,12,13] It is well known that the direct detection of DA with plain electrodes, such as carbon and metallic electrodes, is ineffective. To solve this problem, various electrodes based on chemical modification[14–17] have been developed. The fabrication methods for some of these modified electrodes are relatively sophisticated but time-consuming, such as self-assembly, and layer-by-layer immobilization methods. Therefore, it is still very necessary to develop simple and rapid modification methods to construct sensitive and selective biosensors for the detection of DA.

The detection of DA on a bare glassy carbon electrode (GCE) suffers interference from ascorbic acid (AA) and other biomolecules, such as uric acid (UA). In order to improve the selectivity of the sensor, it is essential to remove unwanted signals that are generated by interferences. Therefore, an appropriate material for preparing the modified electrode for removing interference is generally required.

Graphene, a single-atom-thick and two-dimensional carbon material, has captured worldwide interest due to its high electrical conductivity, high surface-to-volume ratio, high electron transfer rate and exceptional thermal stability.[18,19] It has been reported that graphene showed good prospects as a potential electrode material in recent years.[20–24] However, the detection of DA on a graphene-modified electrode still suffers interference from AA and UA. Graphene-based nanocomposites have been used for the selective detection of DA. Li and his group utilize a graphene-chitosan

[a]*Key Laboratory of Chemical Biology & Traditional Chinese Medicine Research (Ministry of Education, China), College of Chemistry and Chemical Engineering, Hunan Normal University, Changsha 410081, P. R. China. E-mail: haitaoli_64@yahoo.cn; liu_meiling@126.com; Fax: +86-731-88872046; Tel: +86-731-88872309*
[b]*Hunan Vocational Institute of Safety & Technology, Changsha 410151, P. R. China*

† Electronic supplementary information (ESI) available. See DOI: 10.1039/c2an35708a

modified electrode to selectively detect DA.[20] EDTA-modified reduced graphene (EDTA-RG) was used to prepare the EDTA-RG-Nafion modified electrode for DA detection. The selectivity of these modified electrodes was significantly better than that of the bare GC, Nafion and Nafion-graphene-coated electrodes.[25] Graphene nanocomposites, such as the graphene/Au nanocomposite,[26] and Pt nanoparticles/polyelectrolyte-functionalized ionic liquid (PFIL)/graphene sheets (GS) nanocomposite[27] have been used to construct modified electrodes for DA detection. Therefore, one of the key issues in developing sensitive and selective biosensors is to develop an excellent nanocomposite for fabrication of the modified electrodes.

Ferrocene and its derivatives are well-known as electron mediators[28–34] due to their relatively good electrochemical reversibility, regeneration at low potential, and generation of stable redox forms. It was reported that ferrocene has the capability of catalyzing the oxidation or reduction of many small molecules, such as peroxides,[35] DNA,[36] glucose and AA.[37] However, there are still several challenges concerning the immobilization of ferrocene and its derivatives on the electrode surface, especially for soluble mediators, because they can easily diffuse away from the electrode surface into the bulk solution. Therefore, the leakage of electron-shuttling mediators is a main problem for the modified electrodes. This problem can be resolved by covalent linkage of the mediators with polymer chains, high molecular weight compounds or nanoparticles to build novel redox-active hybrid complexes.[31,32,38–40] Based on these concerns, a ferrocene–bovine serum albumin, multiwall carbon nanotube and ormosil composite has been used to construct a hydrogen peroxide biosensor.[41] An electrochemically deposited nanocomposite of chitosan–Fc/AuNPs/GOx for a glucose biosensor was fabricated.[42] An amperometric enzyme electrode for glucose has been prepared by immobilizing glucose oxidase in ferrocene–cobaltocenium dendrimers.[43] Functionalized carbon nanotube with ferrocene derivatives through covalent coupling and π-stacking was utilized for glucose biosensing.[44] 6-Ferrocenylhexanethiol ($HS(CH_2)_6Fc$) functionalized Fe_3O_4@Au nanoparticles (NPs) were successfully immobilized on the surface of a carbon paste electrode and used for the detection of DA.[45]

Enlightened by these studies, graphene and a new ferrocene derivative were utilized to construct a novel DA biosensor. The new amine-terminated ferrocene derivative (Fc-NH_2) was firstly synthesized by introducing an oligo(phenylene-ethynylene) (OPE) chain and tailoring with an amino and a ferrocene head group. Compared with the aliphatic chain, the OPE chain has a lower resistance.[41,46] Therefore, Fc-NH_2 should have a high electric conductivity and can effectively promote the electron transfer between the ferrocene unit and the substrate. At the same time, the Fc-NH_2 can be conveniently covalently or non-covalently bonded with graphene by hydrogen bonding, electrostatic and π-stacking to form a stable composite and effectively prevent leakage of the ferrocene from the matrix. The novel graphene/Fc-NH_2 nanocomposite combined with Nafion film was used to prepare the Nafion/graphene/Fc-NH_2/GCE for the sensitive and selective detection of DA. The presence of the Nafion and ferrocene derivative in the graphene composite not only provides an excellent environment for DA oxidation but also acts as a barrier to prevent AA from interfering in the DA detection.

2. Experimental

2.1. Apparatus and reagents

A Varian-500 high resolution NMR spectrometer (Bruker AVANCE DRX500, Switzerland), Thermo-Finnigan LCQ-Advantage mass-spectrometer (GCMS-QP2010, Japan), UV-2450 spectrophotometer (Shimadzu, Japan) equipped with 1.0 ml quartz cells, and a Nicolet 670 IR spectrophotometer (Nicolet, USA), were used to confirm the structure of the new compounds. TEM (J-2010TEM, Japan) was utilized to characterize the graphene/Fc-NH_2 nanocomposite. A JEM-6700F field emission scanning electron microscope (JEM-6700F, Japan) was used to characterize the surface of the modified electrode. Electrochemical experiments were performed on a CHI 660C electrochemical workstation (CH Instruments, Shanghai, China). A three-electrode system was employed, including a GCE (or modified GCE), a carbon rod and a saturated calomel electrode (SCE), which served as the working electrode, counter electrode and reference electrode, respectively. All potentials here are cited *versus* SCE.

1-[(4-Amino)phenylethynyl]ferrocene (Fc-NH_2) and ferrocenyl phenylene-ethynylene aniline (Fc-OPE) were firstly synthesized according to the synthesis route as shown in Scheme S1† and the detailed procedures were addressed in the ESI.† These new compounds were thoroughly characterized by NMR, mass spectrum and FT-IR spectroscopy. (1,4-Bis(4-aminophenylethynyl)benzene) (OPE_1) and (4,4′-(4,4′-(ethyne-1,2-diyl) bis(4,1-phenylene))bis(ethyne-2,1-diyl)dibenzenamine) (OPE_2) were synthesized by us as reported elsewhere.[47]

DA and Nafion were purchased from Sigma and used as received. Nafion solution was dissolved in ethanol to prepare a 0.5% solution. All other chemicals were of analytical grade and doubly distilled water was used throughout. 0.1 M phosphate buffer solutions (PBS) were prepared from 0.1 M NaH_2PO_4, 0.1 M Na_2HPO_4 and 0.1 M K_2SO_4. The serum and urine samples were obtained from healthy volunteers.

2.2. Preparation of the Fc-NH_2/graphene composite

Graphene was synthesized according to the modified Hummer's method[48–50] and the main procedures were shown in the ESI.† A certain volume of 2 mM Fc-NH_2 (ethanol) solution was mixed with a certain volume of 1 mg mL^{-1} graphene (aqueous), sonicated for 30 min, and shaken for at least 8 h to form a stable and uniform black solution. And the solution was stable for at least 4 weeks in a refrigerator at 4 °C.

2.3. Preparation and characterization of modified electrodes

Procedures of the electrode preparation include three steps: pretreatment of GCE, immobilization of graphene/Fc-NH_2 and protecting by Nafion film on the electrode surface (shown in Scheme 1). (1) A GCE (CH instruments), 3 mm in diameter, was sequentially polished with 1, 0.3 and 0.05 μm alumina powder, and sonicated in 6.0 M nitric acid/doubly distilled water and ethanol/doubly distilled water for 20 min, respectively. Then, the GCE was subjected to cyclic scanning in 0.2 M H_2SO_4 solution in the potential range from −0.1 V to 1.2 V. When the cyclic voltammogram was almost unchanged, the electrode was taken out,

cleaned with water and dried under a stream of nitrogen. (2) 5 μL of graphene/Fc-NH_2 nanocomposite was dropped onto the surface of the pretreated GCE and dried in air. (3) 5 μL of 0.5% Nafion ethanol solution was coated on the surface of the graphene/Fc-NH_2/GCE and dried in air to obtain the Nafion/graphene/Fc-NH_2/GCE.

2.4. Detection of DA at the modified electrodes

5 mL of 0.1 M PBS was added into an electrochemical cell, and then the three-electrode system was installed in it. Cyclic voltammetry (CV) was performed at 50 mV s^{-1} in the range from −0.10 to 0.50 V after a certain volume of stock DA solution was added into the electrochemical cell. The differential pulse voltammogram (DPV) was recorded from 0 to 0.5 V with the parameters of increment potential, 0.004 V; pulse amplitude, 0.05 V; pulse width, 0.05 s; sample width, 0.0167 s; pulse period, 0.2 s; quiet time, 2 s.

3. Results and discussion

3.1. Characterization of Fc-NH_2 and the Nafion/graphene/Fc-NH_2/GCE

Fig. 1A shows the CV of the GCE in 0.9 mM Fc-NH_2 solution (CH_3CN, containing 0.1 M $LiClO_4$ as electrolyte). A pair of peaks at 0.476/0.394 V was observed and the peak-to-peak separation potential (ΔE_p) value was 82 mV for Fc-NH_2 (a). The peaks can be attributed to the oxidation and reduction of Fc^+/Fc. Due to the attachment of the electron-withdrawing ethynylene unit C≡C, the oxidation potentials of Fc-NH_2 are shifted to higher potentials compared with that of ferrocene. The diffusion coefficient of the novel ferrocene derivative can be estimated according to the following Randles–Sevcik equation:[51]

$$i_p = 2.69 \times 10^5 n^{3/2} A C D^{1/2} v^{1/2}$$

where i_p is the peak current (A), n is the number of electrons transferred in the electrode reaction per mole of the active species, A is the area of electrode (cm^2), D is the diffusion coefficient (cm^2 s^{-1}), v is the scan rate (V s^{-1}), and C represents the concentration of solution (M). To determine D, the effective surface area was calculated using 1 mM $K_3Fe(CN)_6$ as a standard. The experimental results were shown in the ESI (Fig. S1†). For 1 mM $K_3Fe(CN)_6$ in 0.1 M KCl solution, $n = 1$, $D = 7.6 \times 10^{-6}$ cm^2 s^{-1} (ref. 52) and A can be calculated to be 0.089 cm^2. When the CVs were conducted in 1 mM Fc-NH_2 at different scan rates, according to the equation and the relationship between i_p and $v^{1/2}$, D can be calculated to be 7.8×10^{-7}. The diffusion coefficient was considerably smaller than that of ferrocene (4.7×10^{-6})[51] owing to the higher molecular weight of Fc-NH_2.

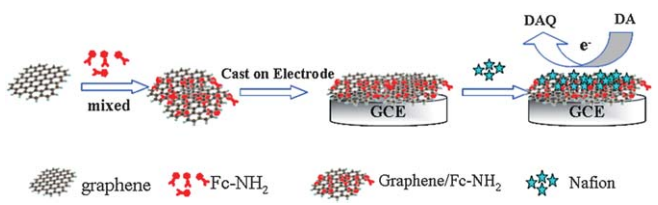

Scheme 1 Schematic illustration of the preparation procedures of the Fc-NH_2 modified electrode.

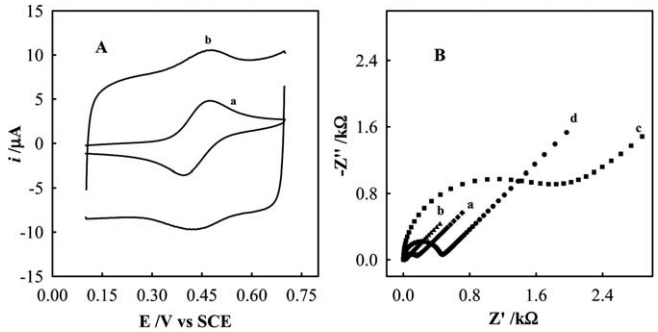

Fig. 1 (A) CVs of GCE in 0.9 mM Fc-NH_2 and Nafion/graphene/Fc-NH_2/GCE in CH_3CN (0.1 M $LiClO_4$ as electrolyte). Scan rate: 50 mV s^{-1}. (B) The electrochemical impedance spectra of Nafion/GCE (a), Nafion/graphene/GCE (b), Nafion/Fc-NH_2/GCE (c), and Nafion/graphene/Fc-NH_2/GCE (d) in 2 mM $K_3Fe(CN)_6$ (containing 0.2 M Na_2SO_4). The applied potential: 0.22 V.

For the Nafion/graphene/Fc-NH_2/GCE (b), a pair of redox peaks at 0.478/0.418 V appeared, and they can be ascribed to the oxidation of Fc-NH_2. It proved that Fc-NH_2 existed in the modified electrode. The modified electrode shows a large capacitance current and a relatively small ΔE_p value compared with that of Fc-NH_2. This is because graphene can accelerate the electron transfer, which resulted in a decrease of ΔE_p. It is reported that several active functional groups in graphene, such as carbonyl groups and carboxyl groups, can enhance the electron transfer.[53] In addition, it is found that the Nafion/graphene/Fc-NH_2/GCE is extremely stable during continuous potential cycling in the range from 0.1 to 0.7 V for 30 cycles. These results indicated that the immobilization of Fc-NH_2 in graphene might efficiently prevent leakage of the mediators. It was reported that carbon nanotubes can interact with ferrocene through

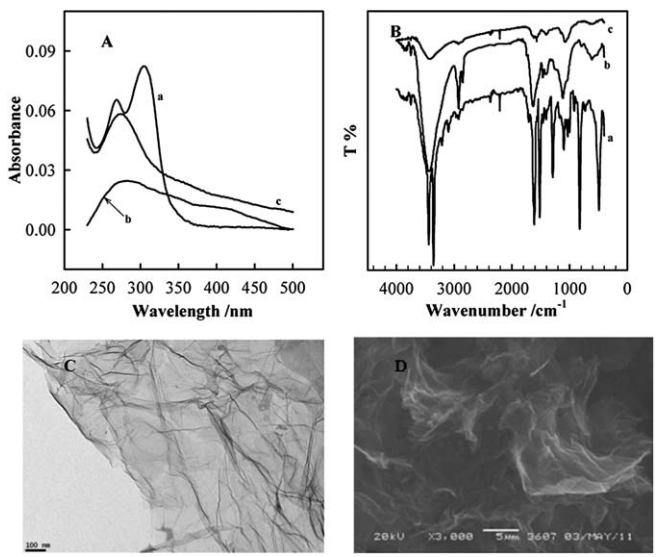

Fig. 2 (A) UV and (B) IR spectra of Fc-NH_2 (a), graphene (b), and graphene/Fc-NH_2 (c). (C) The TEM image of graphene/Fc-NH_2. (D) The SEM image of Nafion/graphene/Fc-NH_2/GCE.

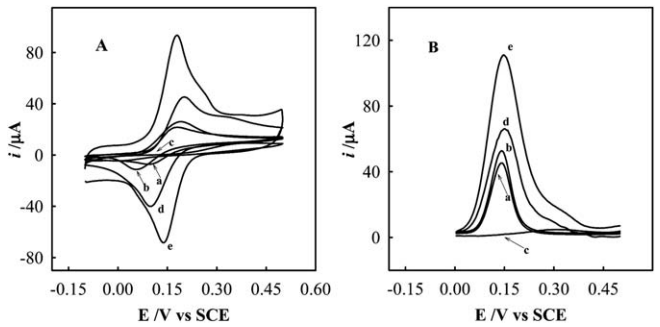

Fig. 3 CVs (A) and DPVs (B) of the GCE (a), Nafion/GCE (b), Fc-NH_2/GCE (c), Nafion/graphene/GCE (d), and Nafion/graphene/Fc-NH_2/GCE (e) in 0.1 M PBS containing 1 mM DA. Scan rate was set at 50 mV s^{-1} in the CV measurements.

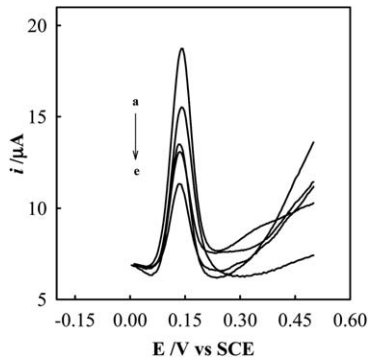

Fig. 4 DPVs of the Nafion/graphene/Fc-NH_2/GCE (a), Nafion/graphene/Fc-OPE/GCE (b), Nafion/graphene/Fc/GCE (c), Nafion/graphene/OPE_2/GCE (d), and Nafion/graphene/OPE_1/GCE (e) in 0.1 M PBS containing 0.1 mM DA.

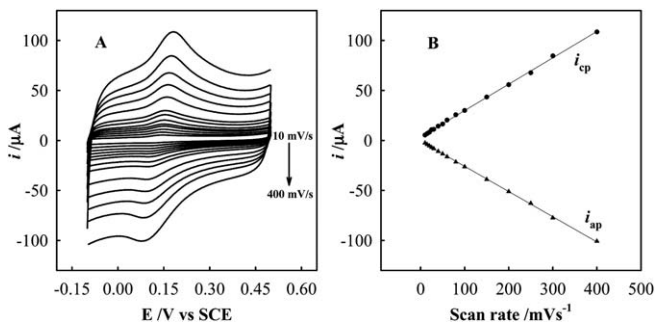

Fig. 5 (A) CVs of the Nafion/graphene/Fc-NH_2/GCE in 0.1 mM DA in 0.1 M PBS (pH 7.0) at different scan rates (from inner to outer: 10, 15, 20, 30, 40, 50, 60, 80, 100, 150, 200, 300, 400 mV s^{-1}). (B) The relationship between peak currents and scan rates.

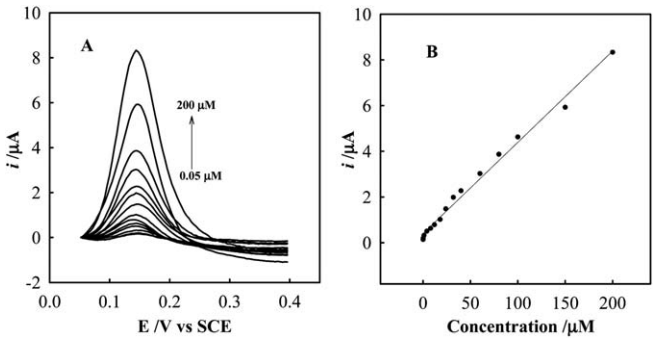

Fig. 6 (A) DPVs of the Nafion/graphene/Fc-NH_2/GCE in various concentrations of DA. Concentrations from 0.050 to 200.00 μM in pH 7.0 PBS. (B) The relationship between the current and concentration of DA.

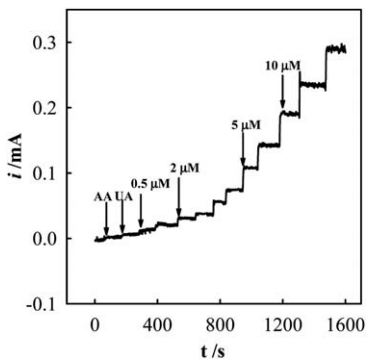

Fig. 7 Current–time response of the Nafion/graphene/Fc-NH_2/GCE for successive addition of AA (1 mM), UA (1 mM) and DA in the concentration range from 0.5 to 10.0 μM in 0.1 M pH 7.0 PBS.

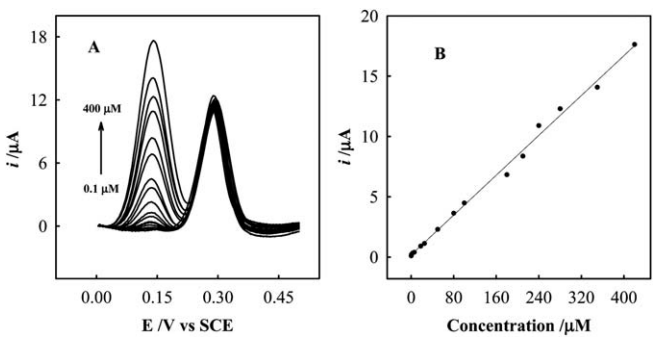

Fig. 8 (A) DPVs of the Nafion/graphene/Fc-NH_2/GCE in various concentrations of DA in pH 7.0 PBS in the presence of 1 mM AA + 0.1 mM UA. (B) The relationship between current and concentration of DA from 0.1 to 400 μM.

π-stacking.[44] And in this work, graphene and Fc-NH_2 might form a stable composite by π-stacking and hydrogen bonding, which can steadily immobilize Fc-NH_2 on the electrode.

Electrochemical impedance spectroscopy (EIS) is an effective method for probing the interfacial properties of modified electrodes. Fig. 1B shows the EIS spectra of Nafion/GCE (a), Nafion/graphene/GCE (b), Nafion/Fc-NH_2/GCE (c), and Nafion/graphene/Fc-NH_2/GCE (d) in 2 mM $K_3(FeCN)_6$. The EI spectra were measured at the formal potential of the electrochemical probe. The semi-circle diameter of the impedance spectrum represents the electron-transfer resistance[54] which controls the electron-transfer kinetics of the redox probe at the electrode interface. It can be seen that Nafion/GCE shows a small semi-circle with the R_{et} of 213 Ω (a). For the Nafion/graphene/GCE (b), the impedance spectrum exhibited an almost straight line, which is the characteristic of a diffusion-limited

Table 1 Determination of DA levels in real samples using the Nafion/graphene/Fc-NH_2/GCE

Sample	Analyte	Detected/μM	Added/μM	Found/μM	Recovery (%)	RSD (%)
Serum 1	DA	—	15	14.6 ± 1.5	97.3	1.5
Urine 1	DA	—	15	14.8 ± 1.1	98.7	1.1
Urine 2	DA	1.5	20	21.6 ± 1.6	102.5	1.6

electrochemical process. When Fc-NH_2 was immobilized under the Nafion film (c), the EI spectrum showed a larger interfacial resistance (2340 Ω), which indicated the successful immobilization of Fc-NH_2 on the electrode surface. For the Nafion/graphene/Fc-NH_2/GCE (d), R_{et} decreased to 488 Ω, and it is larger than that of the Nafion/graphene/GCE. The reason behind this phenomenon may be that the doping of Fc-NH_2 into the modified film somewhat hampered the electron-transfer.

The formation of the graphene/Fc-NH_2 nanocomposite was confirmed by UV and FTIR results. The UV spectra of graphene, Fc-NH_2 and graphene/Fc-NH_2 composite are shown in Fig. 2A. Graphene (b) shows a broad peak at 278 nm and the Fc-NH_2 (a) shows two peaks at 260 and 305 nm. For the graphene/Fc-NH_2 nanocomposite (c), a peak at 270 nm appeared. Owing to the small ratio of Fc-NH_2 in the graphene/Fc-NH_2 composite, the characteristic peaks of Fc-NH_2 were covered up by graphene. While the peak of graphene was somewhat blue shifted, and this may result from the π-stacking between graphene and Fc-NH_2. Fig. 2B shows the FT-IR spectra of graphene, Fc-NH_2 and the graphene/Fc-NH_2 composite. Compared to the bands in the spectra of Fc-NH_2 (a) and graphene (b), the characteristic bands of ferrocene appeared at 2926, 1406, 1106, 1043 and 810 cm^{-1} in the spectrum of graphene/Fc-NH_2 (c). And the C≡C of Fc-NH_2 was obviously observed in the spectrum of graphene/Fc-NH_2 (c). Therefore, the graphene/Fc-NH_2 composite was successfully formed.

The TEM image of graphene/Fc-NH_2 is shown in Fig. 2C. It is very clear that Fc-NH_2 was well dispersed on the flake-like graphene sheet. The SEM image of the Nafion/graphene/Fc-NH_2/GCE is shown in Fig. 2D. It can be seen that a crumpled, wrinkled and layered structure of the graphene sheet was formed on the surface of the GCE.

3.2. Electro-oxidation of DA at the modified GCE

Since the modified electrode exhibits a stable and reversible electrochemical response, it can be used as a sensor platform to detect small molecules. DA was selected as a model system to evaluate the performance of the modified electrodes. The CVs and DPVs of bare GCE (a), Nafion/GCE (b), Fc-NH_2/GCE (c), Nafion/graphene/GCE (d) and Nafion/graphene/Fc-NH_2/GCE (e) in 0.1 M PBS (pH 7.0) containing 1 mM DA are shown in Fig. 3. The bare GCE shows a pair of peaks near 0.2 V, and it can be attributed to the oxidation of DA into DAQ.[55] The oxidation peak potential (E_{pa}) of the Nafion/GCE (b) located near 0.20 V and the higher redox current was obtained. A broad, ill-defined redox peak of DA was observed at 0.4 V for the Fc-NH_2/GCE (c). The increases in oxidation currents of DA at the Nafion/graphene/GCE and Nafion/graphene/Fc-NH_2/GCE are observed in the presence of graphene and Fc-NH_2. And the DPVs (Fig. 3B) results are in agreement with the CV measurements. The largest current response on the Nafion/graphene/Fc-NH_2/GCE may be ascribed to three factors. Firstly, the presence of graphene can significantly enlarge the active surface area of the electrode and several active functional groups on the surface of graphene, such as carbonyl groups and carboxyl groups, can act as media to enhance the electron transfer and catalyze the oxidation of DA.[53] Secondly, Fc-NH_2 is an excellent mediator for accelerating the electron transfer between the Nafion/graphene/Fc-NH_2/GCE and solution. The enhancement of current may come from the synergy effect of graphene and Fc-NH_2. Both graphene and Fc-NH_2 coexist in the modified electrode, and the best amplifying effect can be obtained. Thirdly, Nafion not only acts as an anion barrier but also acts as a functional film for accumulation of the positively charged molecules. Unwin's group reported that trimethylammonium ferrocenium can transport into ultrathin Nafion Langmuir Schaefer films.[56,57] This result is different from the present research. In this work, positively charged Fc-NH_2 was reacted with graphene to form a complex, which led to it hardly diffusing away from the complex into the Nafion film. The positively charged DA molecules were gathered from the solution through the anionic sulfuric groups of the Nafion structures.[58] Therefore, Nafion on the Nafion/graphene/Fc-NH_2/GCE can enhance the sensitivity of the modified electrode for DA detection. It is reported that thicker Nafion will result in a higher selectivity but will lower the mass transfer rate of DA.[25] Therefore, a medium-thickness Nafion (5 μL 0.5% Nafion) film was adopted in this work.

To thoroughly investigate the amplification effect of the modified electrode in DA detection, we compared the related ferrocene derivatives and OPE molecules with Fc-NH_2 (as shown in Fig. 4). The modified electrodes prepared by the same procedure as that of the Nafion/graphene/Fc-NH_2/GCE only replaced the Fc-NH_2 with ferrocene, Fc-OPE, OPE_1 and OPE_2. The oxidation currents of DA on all the modified electrodes increased compared with the bare GCE, as can be seen in Fig. 4. The peak potentials were near 0.15 V in all cases though the peak currents were different. The electrodes containing Fc-NH_2 (a) and Fc-OPE (b) have an obviously larger current than other cases. And the current on the graphene/OPE_2 (d) modified electrode was almost the same as that of the graphene/ferrocene modified electrode (c). Therefore, we may conclude that ferrocene and OPE may play important roles in the amplified determination of DA. In the case of graphene/Fc-OPE and graphene/Fc-NH_2 modified electrodes, ferrocene derivatives can accelerate the electron transfer and OPE can act as a good link-bridge. And the amino group also plays an important role, which may also react with carboxyl and hydroxyl in graphene through electrostatic and hydrogen bonding. It is noteworthy that the response of DA on the graphene/Fc-OPE modified electrode was smaller than

that of the graphene/Fc-NH_2 modified electrode. This may result from the larger molecular structure of the Fc-OPE, which could lead to a smaller co-plane of ferrocene and phenylethynyl, and thus decrease the conjugation effect of Fc-OPE to graphene.

To further explore the redox characteristics of DA on the Nafion/graphene/Fc-NH_2/GCE, the effect of scan rate on the redox peak current of DA was investigated in detail. Fig. 5A depicts CVs of the Nafion/graphene/Fc-NH_2/GCE in 0.1 mM DA at the scan rates from 10 to 400 mV s^{-1}. The ΔE_p increased with scan rate, and the relationship of the reduction–oxidation peak currents to the scan rates predicts a kinetic process of the electron transfer between the solution and the electrode. As shown in Fig. 5B, the relationship between redox peak current and scan rate is linear (the linear correlation coefficient is 0.999). These phenomena suggested that there is not enough time for DA to diffuse through the Nafion/graphene/Fc-NH_2 film and the electrochemical redox behavior of DA at the Nafion/graphene/Fc-NH_2/GCE surface is a surface adsorption-controlled process.[59]

3.3. Optimization of conditions

The electrochemical redox behavior of DA on the Nafion/graphene/Fc-NH_2/GCE in different buffer media (such as 0.1 M pH 4.5 HAc–NaAc, pH 7.0 PBS, pH 9.3 $NH_3 \cdot H_2O$–NH_4Cl) was investigated. A pair of well-defined reversible redox waves of DA was observed in PBS, and therefore, 0.1 M PBS (pH 7.0) was adopted to determine DA.

The mass ratio of graphene to Fc-NH_2 and the amount of graphene/Fc-NH_2 nanocomposite on the GCE were also optimized. The relationship between the DPV oxidation peak currents (I) and the mass ratios of graphene to Fc-NH_2 was shown in Fig. S2A.† It was found that the ratio of 20 : 1 was the best. Though the Fc-NH_2 can act as a mediator to accelerate the electron transfer, excessive amounts of Fc-NH_2 may decrease the conductivity of the graphene/Fc-NH_2 nanocomposite.

The amount of graphene/Fc-NH_2 on a GCE was investigated. As shown in Fig. S2B,† the current obviously increased when the amount of graphene/Fc-NH_2 was increased from 2 to 5 μL, and then increased slightly from 5 to 6 μL. When the amount exceeded 10 μL, the current decreased dramatically. It may be ascribed to the thick film of graphene/Fc-NH_2 somewhat hampering the electrical conductivity. Therefore, the volume of graphene/Fc-NH_2 suspension was chosen at 5 μL in this work.

3.4. Detection of DA on Nafion/graphene/Fc-NH_2/GCE

Under the optimized conditions, DA was detected with DPV in 0.1 M PBS (pH 7.0). In this process, the Nafion/graphene/Fc-NH_2/GCE was cleaned with voltammetric cycles in pH 7.0 PBS after every measurement so as to renew the electrode surface. The experimental results showed that the peak current increased with concentration of DA and the peak potential remained unchanged. As shown in Fig. 6B, the peak height of the DPV current is linearly related to the DA concentration in the range of 0.05–200 μM. The detection limit was 0.02 μM at a signal to noise of 3, and it was much lower than those reported previously (0.64 μM,[45] 2.64 μM,[27] 25 μM[60]). This new material should have potential application in constructing a sensitive DA biosensor.

3.5. Inference of detection of DA

Based on the voltammetric results described above, the amperometric current–time response of the Nafion/graphene/Fc-NH_2/GCE was recorded with successive addition of DA, AA and UA in stirred PBS. As shown in Fig. 7, the current response was rapid when DA was added in the test solution and reached a steady state (95% of the maximum value) within 3 s, indicating that the biosensor possessed high sensitivity to DA. When the AA and UA concentration was 1000 and 100 times higher than DA, respectively, almost no current response was observed. Therefore, the Nafion/graphene/Fc-NH_2/GCE can be utilized to selectively determine DA.

3.6. Selective determination of DA in the presence of AA and UA

The detection of DA in the presence of AA and UA was also conducted. CVs of the Nafion/graphene/Fc-NH_2/GCE in PBS with different concentrations of DA, AA and UA were shown in Fig. S3 in the ESI.† There is no oxidation peak for AA in the CV curve, while two oxidation peaks near 0.15 and 0.35 V were observed for DA and UA, respectively. AA is negatively charged at pH 7.0 and Nafion acts as an anion barrier which can prevent the electro-oxidation of AA. And the oxidation peak of DA in the DPV curve remains constant at 0.15 V with the addition of UA and AA.

Fig. 8A illustrates a series of DPVs obtained at different concentrations of DA in the presence of 1 mM AA and 0.1 mM UA at the Nafion/graphene/Fc-NH_2/GCE. Two peaks in the DPV curves were observed, which were associated with the oxidation of DA and UA. In these curves, the oxidation peak of AA did not appear. And the peak of UA almost remained unchanged with the increase in DA concentration. Fig. 8B shows the relationship between the peak current and the concentration of DA. The peak height is linearly related to DA concentration in the range of 0.1–400 μM. The detection limit was 0.05 μM at a signal-to-noise ratio of 3, and it was much lower than those reported previously.[20] Our results demonstrate that the presence of over an 1000 times concentration of AA and an 100 times concentration of UA do not interfere with the anodic peak of DA on the electrode surface. It is predicted that DA can be selectively detected in bio-samples with this new modified electrode.

3.7. Real samples analysis

The applicability of the modified electrode was tested by measuring real samples, such as serum and urine samples using the standard addition method. In order to avoid the interferences from the matrix in real samples and to fit into the linear range of DA, low concentrations of urine and serum samples were used. To ascertain the correctness of the results, the diluted sample mentioned above was spiked with certain amount of DA and then detected. The recovery of the spiked samples ranged between 97 and 103% (Table 1).

4. Conclusion

In this paper, a new ferrocene derivative, 1-[(4-amino)phenylethynyl]ferrocene (Fc-NH_2) was synthesized for the first time.

The new Fc-NH_2 has excellent electrochemical properties. A highly sensitive and selective biosensor can be fabricated by using the complex of Fc-NH_2 and graphene. The biosensor showed good selectivity and sensitivity to DA detection with a wide linear range and without any interference from at least two orders-of-magnitude higher concentrations of AA and UA than DA. Therefore, it highlights a promising use of the nanomaterial and the new ferrocene mediator complex in the construction of new biosensors.

Acknowledgements

This work was supported by the National Natural Science Foundation of China (20975037 and 201075037) and the Scientific Research Fund of Hunan Provincial Education Department (10C0926, CX2010b218) and Aid Program for Science and Technology Innovative Research Team in Higher Educational Institutions of Hunan Province.

References

1 K. Pihel, Q. D. Walker and R. M. Wightman, *Anal. Chem.*, 1996, **68**, 2084–2089.
2 C. S. Cha, J. Chen and P. F. Liu, *Biosens. Bioelectron.*, 1998, **13**, 87–94.
3 J. Kehr, X. J. Hu, T. Yoshitake and D. Scheller, *J. Chromatogr., B: Anal. Technol. Biomed. Life Sci.*, 2007, **845**, 109–113.
4 K. Thorré, M. Pravda, S. Sarre, G. Ebinger and Y. Michotte, *J. Chromatogr., B: Biomed. Sci. Appl.*, 1997, **694**, 297–303.
5 L. Zhang, N. Teshima, T. Hasebe, M. Kurihara and T. Kawashima, *Talanta*, 1999, **50**, 677–683.
6 L. Li, H. Liu, Y. Shen, J. Zhang and J.-J. Zhu, *Anal. Chem.*, 2011, **83**, 661–665.
7 Y. Wang and H. Chen, *J. Chromatogr., A*, 2005, **1080**, 192–198.
8 M. Shou, C. R. Ferrario, K. N. Schultz, T. E. Robinson and R. T. Kennedy, *Anal. Chem.*, 2006, **78**, 6717–6725.
9 R. Baron, M. Zayats and I. Willner, *Anal. Chem.*, 2005, **77**, 1566–1571.
10 G. Fabregat, E. Córdova-Mateo, E. Armelin, O. Bertran and C. Alemán, *J. Phys. Chem. C*, 2011, **115**, 14933–14941.
11 D. Lakshmi, A. Bossi, M. J. Whitcombe, I. Chianella, S. A. Fowler, S. Subrahmanyam, E. V. Piletska and S. A. Piletsky, *Anal. Chem.*, 2009, **81**, 3576–3584.
12 T. Selvaraju and R. Ramaraj, *Electrochem. Commun.*, 2003, **5**, 667–672.
13 M. Zhang, K. Gong, H. Zhang and L. Mao, *Biosens. Bioelectron.*, 2005, **20**, 1270–1276.
14 H. Mao and P. G. Pickup, *J. Electroanal. Chem. Interfacial Electrochem.*, 1989, **265**, 127–142.
15 S. A. Wring, J. P. Hart and B. J. Birch, *Anal. Chim. Acta*, 1990, **229**, 63–70.
16 M. E. G. Lyons, W. Breen and J. Cassidy, *J. Chem. Soc., Faraday Trans.*, 1991, **87**, 115–123.
17 J. M. Leal, P. L. Domingo, B. Garcia and S. Ibeas, *J. Chem. Soc., Faraday Trans.*, 1993, **89**, 3571–3577.
18 E. Jin, X. Lu, L. Cui, D. Chao and C. Wang, *Electrochim. Acta*, 2010, **55**, 7230–7234.
19 P. Wu, Q. Shao, Y. Hu, J. Jin, Y. Yin, H. Zhang and C. Cai, *Electrochim. Acta*, 2010, **55**, 8606–8614.
20 Y. Wang, Y. Li, L. Tang, J. Lu and J. Li, *Electrochem. Commun.*, 2009, **11**, 889–892.
21 S. Alwarappan, A. Erdem, C. Liu and C. Z. Li, *J. Phys. Chem. C*, 2009, **113**, 8853–8857.
22 X. Kang, J. Wang, H. Wu, I. A. Aksay, J. Liu and Y. Lin, *Biosens. Bioelectron.*, 2009, **25**, 901–905.
23 C. Shan, H. Yang, J. Song, D. Han, A. Ivaska and L. Niu, *Anal. Chem.*, 2009, **81**, 2378–2382.
24 C. Shan, H. Yang, D. Han, Q. Zhang, A. Ivaska and L. Niu, *Langmuir*, 2009, **25**, 12030–12033.
25 S. Hou, M. L. Kasner, S. Su, K. Patel and R. Cuellari, *J. Phys. Chem. C*, 2010, **114**, 14915–14921.
26 C. Fu, Y. Kuang, Z. Huang, X. Wang, N. Du, J. Chen and H. Zhou, *Chem. Phys. Lett.*, 2010, **499**, 250–253.
27 F. Li, J. Chai, H. Yang, D. Han and L. Niu, *Talanta*, 2010, **81**, 1063–1068.
28 P. Marianne, *Anal. Chim. Acta*, 1986, **187**, 333–338.
29 J. Kulys and E. J. D'Costa, *Anal. Chim. Acta*, 1991, **243**, 173–178.
30 A. Escorcia and A.-A. Dhirani, *J. Electroanal. Chem.*, 2007, **601**, 260–268.
31 J. Qiu, H. Peng and R. Liang, *Electrochem. Commun.*, 2007, **9**, 2734–2738.
32 J. D. Qiu, J. Guo, R. P. Liang and M. Xiong, *Electroanalysis*, 2007, **19**, 2335–2341.
33 T. T. Hien Pham, C. Cao and S. J. Sim, *J. Magn. Magn. Mater.*, 2008, **320**, 2049–2055.
34 L. Fernández and H. Carrero, *Electrochim. Acta*, 2005, **50**, 1233–1240.
35 M. A. Rampi, O. J. A. Schueller and G. M. Whitesides, *Appl. Phys. Lett.*, 1998, **72**, 1781–1783.
36 D. J. Wold, R. Haag, M. A. Rampi and C. D. Frisbie, *J. Phys. Chem. B*, 2002, **106**, 2813–2816.
37 A. Callegari, M. Marcaccio, D. Paolucci, F. Paolucci, N. Tagmatarchis, D. Tasis, E. Vazquez and M. Prato, *Chem. Commun.*, 2003, 2576–2577.
38 Y. Okawa, M. Nagano, S. Hirota, H. Kobayashi, T. Ohno and M. Watanabe, *Biosens. Bioelectron.*, 1999, **14**, 229–235.
39 T. Masuko, A. Minami, N. Iwasaki, T. Majima, S.-I. Nishimura and Y. C. Lee, *Biomacromolecules*, 2005, **6**, 880–884.
40 J. Chen, J. Tang, F. Yan and H. Ju, *Biomaterials*, 2006, **27**, 2313–2321.
41 V. B. Kandimalla, V. S. Tripathi and H. Ju, *Biomaterials*, 2006, **27**, 1167–1174.
42 J. D. Qiu, R. Wang, R. P. Liang and X. H. Xia, *Biosens. Bioelectron.*, 2009, **24**, 2920–2925.
43 B. Alonso, P. G. A. Armada, J. Losada, I. Cuadrado, B. González and C. M. Casado, *Biosens. Bioelectron.*, 2004, **19**, 1617–1625.
44 A. L. Goff, F. Moggia, N. Debou, P. Jegou, V. Artero, M. Fontecave, B. Jousselme and S. Palacin, *J. Electroanal. Chem.*, 2010, **641**, 57–63.
45 J. Qiu, M. Xiong, R. Liang, H. Peng and F. Liu, *Biosens. Bioelectron.*, 2009, **24**, 2649–2653.
46 A. Callegari, S. Cosnier, M. Marcaccio, D. Paolucci, F. Paolucci, V. Georgakilas, N. Tagmatarchis, E. Vazquez and M. Prato, *J. Mater. Chem.*, 2004, **14**, 807–810.
47 J. Luo, M. Liu, Q. Zhao, J. Zhao, Y. Zhang, L. Tan, H. Tang, Q. Xie, H. Li and S. Yao, *Electrochim. Acta*, 2010, **56**, 454–462.
48 W. S. Hummers and R. E. Offeman, *J. Am. Chem. Soc.*, 1958, **80**, 1339.
49 N. I. Kovtyukhova, P. J. Ollivier, B. R. Martin, T. E. Mallouk, S. A. Chizhik, E. V. Buzaneva and A. D. Gorchinskiy, *Chem. Mater.*, 1999, **11**, 771–778.
50 M. Kim, N. S. Safron, E. Han, M. S. Arnold and P. Gopalan, *Nano Lett.*, 2010, **10**, 1125–1131.
51 T. Morikita and T. Yamamoto, *J. Organomet. Chem.*, 2001, **637-639**, 809–812.
52 H. Yin, Q. Ma, Y. Zhou, S. Ai and L. Zhu, *Electrochim. Acta*, 2010, **55**, 7102–7108.
53 D. L. Robinson, A. Hermans, A. T. Seipel and R. M. Wightman, *Chem. Rev.*, 2008, **108**, 2554–2584.
54 C. Hortholary and C. Coudret, *J. Org. Chem.*, 2003, **68**, 2167–2174.
55 Y. Li, M. Liu, C. Xiang, Q. Xie and S. Yao, *Thin Solid Films*, 2006, **497**, 270–278.
56 P. Bertoncello, I. Ciani, F. Li and P. R. Unwin, *Langmuir*, 2006, **22**, 10380–10388.
57 P. Bertoncello, I. Ciani, D. Marenduzzo and P. R. Unwin, *J. Phys. Chem. C*, 2007, **111**, 294–302.
58 S. M. Chen, J. Y. Chen and R. Thangamuthu, *Electroanalysis*, 2007, **19**, 1531–1538.
59 A. J. F. Bard, L. R. Faulkner, *Electrochemical Methods*, John Wiley & Sons, Inc, New York, 1980.
60 S. K. Tembe, B. S. Kubal, M. Karve and S. F. D'Souza, *Anal. Chim. Acta*, 2008, **612**, 212–217.